cis-Retinol/Androgen Dehydrogenase, Isozyme 3 (CRAD3): A Short-Chain Dehydrogenase Active in a Reconstituted Path of 9-*cis*-Retinoic Acid Biosynthesis in Intact Cells[†,‡]

Run Zhuang, Min Lin, and Joseph L. Napoli*

Department of Nutritional Sciences and Toxicology, University of California, Berkeley, California 94720-3104

Received October 15, 2001; Revised Manuscript Received January 18, 2002

ABSTRACT: 9-*cis*-Retinoic acid activates retinoid *X* receptors, which serve as heterodimeric partners with other nuclear hormone receptors, yet the enzymology of its physiological generation remains unclear. Here, we report the identification and molecular/enzymatic characterization of a previously unknown member of the short-chain dehydrogenase/reductase family, CRAD3 (*cis*-retinoid/androgen dehydrogenase, type 3), which catalyzes the first step in 9-*cis*-retinoic acid biosynthesis, the conversion of 9-*cis*-retinol into 9-*cis*-retinal. CRAD3 shares amino acid similarity with other retinoid/steroid short-chain dehydrogenases/reductases: CRAD1, CRAD2, and RDH4. Relative to CRAD1, CRAD3 has greater 9-*cis*-retinol/*all-trans*-retinol discrimination and lower efficiency as an androgen dehydrogenase. CRAD3 has apparent efficiency (V/K_m) for 9-*cis*-retinol about equivalent to that for CRAD1 and 3 orders of magnitude greater than that for RDH4. (CRAD2 does not recognize 9-*cis*-retinol as a substrate). CRAD3 contributes to 9-*cis*-retinoic acid production in intact cells, in conjunction with each of three retinal dehydrogenases that recognize 9-*cis*-retinal (RALDH1/AHD2, RALDH2, and ALDH12). Liver and kidney, two tissues reportedly with the highest concentrations of 9-*cis*-retinoids, show the most intense mRNA expression of CRAD3, but expression also occurs in testis, lung, small intestine, heart, and brain. These data are consistent with the participation of CRAD3 in the biogeneration of 9-*cis*-retinoic acid.

Vertebrates require retinoids biosynthesized from retinol (vitamin A) for vision, reproduction, embryogenesis, intermediary metabolism, and the maintenance of normal epithelia, bone, nerves, and immunity (*1*, *2*). The retinol metabolite atRA[1] satisfies all known retinoid endocrine functions, primarily by activating the three nuclear receptors RARα, *β*, and *γ* (*3*, *4*). The isomer 9cRA controls the distinct receptors RXRα, *β*, and *γ*, which alter functions of several other nuclear receptors through heterodimerization, including RAR, VDR, and PPAR. These heterodimers seem to require only the non-RXR ligand for maximum activation, if present in sufficient concentration. 9cRA increases heterodimer activation when non-RXR ligand concentrations fall below maximum. Nevertheless, 9cRA and its analogues may affect disease progression, including noninsulin-dependent diabetes mellitus (*5*). This suggests that endogenous 9cRA has fundamental effects in vivo and, therefore, that its biogeneration would be controlled. Understanding 9cRA biosynthesis and its control seems essential to understanding the precise functions of RXR and the mechanisms that regulate RXR-controlled genes.

Androgens virilize through programming the formation and maturation of reproductive organs and the development of secondary sex characteristics (*6*). Testes produce the potent androgen testosterone, whereas prostate and other tissues convert testosterone into the potent androgen DHT (*7*). Testosterone directs internal male genitalia formation. DHT programs embryonic external sex organ development and the phenotypic changes of male puberty (*8*). Both testosterone and DHT bind to and activate the androgen receptor. Reduction of its 3-oxo functional group converts DHT into 3-adiol, which lowers its affinity for the androgen receptor 5-fold, greatly reducing its potency as an androgen. SDR can further inactivate 3-adiol through 17*β*-dehydrogenation into the very low-activity androsterone or regenerate DHT from 3-adiol through 3α-dehydrogenation (*9*−*11*).

The SDR enzyme superfamily comprises more than 50 animal enzymes that control the activities of prostanoids, steroids, and retinoids (*12*, *13*). SDR share conserved cofactor binding sites, catalytic residues, and tertiary structures but have relatively few strictly conserved residues. SDR often are multifunctional; each may catalyze metabolism of distinct substrate types. An SDR subfamily, sharing close amino acid identities, catalyzes either *trans*- or *cis*-retinol and androgen dehydrogenation as 3α-HSD. These enzymes could serve in the visual cycle or generate the endocrine factors atRA and 9cRA or to reactivate 3-adiol into DHT (*14*, *15*).

[†] This work was supported, in part, by Grant DK47839 from the NIH.

[‡] The nucleotide sequence of CRAD3 has been submitted to GenBank under accession number AF372838.

* Corresponding author. Phone: 510-642-0908. Fax: 510-642-0535. E-mail: jna@uclink4.berkeley.edu.

[1] Abbreviations: AHD2, mouse aldehyde dehydrogenase, type 2; 3-adiol, 5α-androstan-3α,17*β*-diol; androstanedione, 5α-androstan-3,17-dione; androstenedione, 4-androsten-3,17-dione; androsterone, 5α-androstan-3α-ol-17-one; CRAD, *cis*-retinol/androgen dehydrogenase; DHT, (dihydrotestosterone), 5α-androstan-17*β*-ol-3-one; HSD, hydroxysteroid dehydrogenase; atRA, *all-trans*-retinoic acid; 9cRA, 9-*cis*-retinoic acid; RALDH, retinal dehydrogenase; RDH, retinol dehydrogenase; SDR, short-chain dehydrogenase(s)/reductase(s); testosterone, 4-androsten-17*β*-ol-3-one.

10.1021/bi0119316 CCC: $22.00 © 2002 American Chemical Society
Published on Web 02/14/2002

Here, we report the isolation of a cDNA that encodes a previously unknown SDR (CRAD3), the enzymatic characteristics of CRAD3, and its mRNA expression patterns. CRAD3 has an efficiency (V/K_m) equivalent with that of CRAD1 but a much higher activity than other SDR (CRAD2 and RDH4) that catalyze the dehydrogenation of *cis*-retinols (*16*−*20*). In addition, CRAD3 has lower efficiency as a 3α-HSD than either CRAD1 or CRAD2. CRAD3 functions in intact cells in conjunction with each of three RALDH isomers active with 9-*cis*-retinal to produce 9cRA and is expressed in tissues that express RXR (*14*, *21*, *22*). These characteristics are consistent with CRAD3 contributing to 9-*cis*-retinol metabolism in vivo.

EXPERIMENTAL PROCEDURES

Library Screening. A 129 SvJ mouse genomic DNA library was screened through three rounds with a [^{32}P]labeled 374 base-pair probe consisting of RoDH2 nucleotides 11−384 (*23*). Hybridization was done at 42 °C overnight. Membranes were washed in 2*x*SSC and 0.5% SDS at room temperature for 20 min, followed by two washes in 1*x*SSC and 0.1% SDS at 65 °C for 1 h each time. Five positive plaques were identified. DNA from one was isolated (QIAGEN lambda maxi kit), and digests were analyzed by southern blot with the same probe used for library screening. The smallest fragment generated by digestion with *Eco*RI (2 kb) was subcloned and sequenced. It contained nucleotides 1−394 of the final cDNA of CRAD3.

cDNA Isolation. A ∼2.7 kb EST clone (ATCC no. 1895114) has a sequence identical with that in the 2 kb fragment. The EST insert was resequenced, and its coding region was PCR-amplified with primers identical to the translation start and stop codons. A Kozak sequence, GCCGCCACC, was added to the sense primer immediately before the translation start codon. *Bam*HI and *Xba*I recognition sites (underlined) were added to the 5′ ends of the sense and antisense primers: CGGGATCCGCCGCCACCATGTGGCTCTTTCTAGTGGCACTG and GCTCTAGATCAGAGGGCTTTCTCAGGCTTCAG, respectively. This generated a 979 base-pair fragment, which was cloned into pcDNA3 to produce pcDNA3/CRAD3.

Expression of CRAD3. CHO cells were cultured in Ham's F-12 medium (10 mL) supplemented with 10% fetal calf serum (2×10^6 cells/100 mm dish) at 37 °C under 5% CO_2. Unless stated otherwise, after 24 h (50−80% confluence), cells were transfected with 8 μg DNA/dish of pcDNA3/CRAD3 or pcDNA3 complexed with LipofectAMINE (Life Technologies, Inc.). CHO cells from a single transfection were harvested 24 h later and were lysed by sonication in a lyses buffer (20 mM Hepes, 150 mM KCl, 1 mM EDTA, 10% sucrose, and 2 mM dithiothreitol (pH 7.5)). Kinetic values were obtained with the supernatant produced by a 10 000*g* spin for 10 min.

Enzyme Assays. Unless stated otherwise, retinol and sterol dehydrogenase assays were done with radioinert retinoids or [^{3}H]steroids with 2 mM NAD^+ at 37 °C in 20 mM Hepes, 150 mM KCl, and 1 mM EDTA at pH 8. Initial screening for candidate substrates was done with 10−20 μg of protein and for 10−20 min (i.e., not necessarily under linear conditions). K_m values were obtained under initial velocity conditions (linear rates with protein and time; i.e., at 2−6 μg of protein and 4−10 min). Protein was measured by the method of Bradford (*24*). Products were quantified by HPLC (retinals) or TLC (steroids), as described (*17*). Data were fit with nonlinear regression analyses using the computer program Graph Pad Prism.

CRAD1 versus CRAD3. To compare the activities of CRAD3 and CRAD1, CHO cells were transfected with 8 μg of pcDNA3 (mock transfection), pcDNA3/CRAD3, or pcDNA/CRAD1 and 0.1 μg of the luciferase expression vector pGL3. The 10 000*g* supernatants were used to measure enzyme and luciferase activity. Luciferase activity was measured with the Promega Luciferase Assay System according to the instructions. Data were normalized to transfection efficiencies of 89% for CRAD3 relative to CRAD1.

Whole Cell Assays. CHO cells in six-well tissue culture plates were cotransfected with combinations of pcDNA3 (mock transfection), pcDNA3/CRAD3, pcDNA3/ALDH12, pcDNA3/RALDH, pcDNA3/RALDH2, and the luciferase expression vector pGL3. Twenty-four hours after transfection, 9-*cis*-retinol in dimethyl sulfoxide (5 μL) was added to the cells at a final concentration of 1 μM. One hour later, cells and medium were harvested independently. Cells were lysed in a lyses buffer. Aliquots of the cell lysates were used to measure protein by the Bradford method (*24*) and by luciferase activity, as described previously. To measure 9cRA, 20% of each cell lysate was combined with 20% of its medium to give a total volume of 1.2 mL. To each sample was added 2.5 mL of 0.025N KOH/ethanol, and neutral and basic lipids were extracted with hexane (6 mL). The aqueous phases were acidified with 0.15 mL of 4 N HCl, and 9cRA was extracted with hexane (6 mL). This hexane phase was evaporated with a stream of nitrogen, and the residues were dissolved in hexane (0.1 mL). 9cRA was quantified by normal-phase HPLC eluted with 97% hexane (containing 0.35% acetic acid) and 3% dichloroethane, as described (*22*). Data were normalized to the amount of protein and for transfection efficiencies.

Northern Blot. A 455 base-pair probe corresponding to nucleotides 2170−2625 of CRAD3 was generated by PCR with the sense primer CTCCTCTTCTCTCAGTAG and the antisense primer TATACCCTGCAGCATGAC. The probe was labeled with ^{32}P by random priming and hybridized to a multiple tissue northern blot membrane (Clontech) containing 2 μg of poly(A^+) RNA per lane. Prehybridization was done in 10 mL of ExpressHyb solution at 68 °C for 30 min. Hybridization was done in 15 mL of fresh ExpressHyb solution with a [^{32}P]labeled probe at 68 °C for 1 h. The membrane was washed in 2*x*SSC and 0.05% SDS at room temperature for 40 min and then was washed twice in 0.1*x*SSC and 0.1% SDS at 50 °C for 40 min. Signals were detected by autoradiography.

RT-PCR. Mouse poly(A)+ RNA (250 ng), purchased from Sigma, was used for reverse transcription with the ThermoScript RT-PCR system (Life Technology). cDNAs were diluted 10-fold, and 1 μL of each diluted stock was used. Amplification was done for 2 min at 94 °C and for *X* cycles of 30 s at 94 °C, 30 s at 55 °C, and 40 s at 72 °C (with a final incubation for 7 min at 72 °C) with the same primers used for amplification of the northern probe. Different numbers of cycles were used to define optimal conditions for linearity. The analysis was done with 30 cycles for CRAD3 and 26 cycles for β-actin. As a negative control,

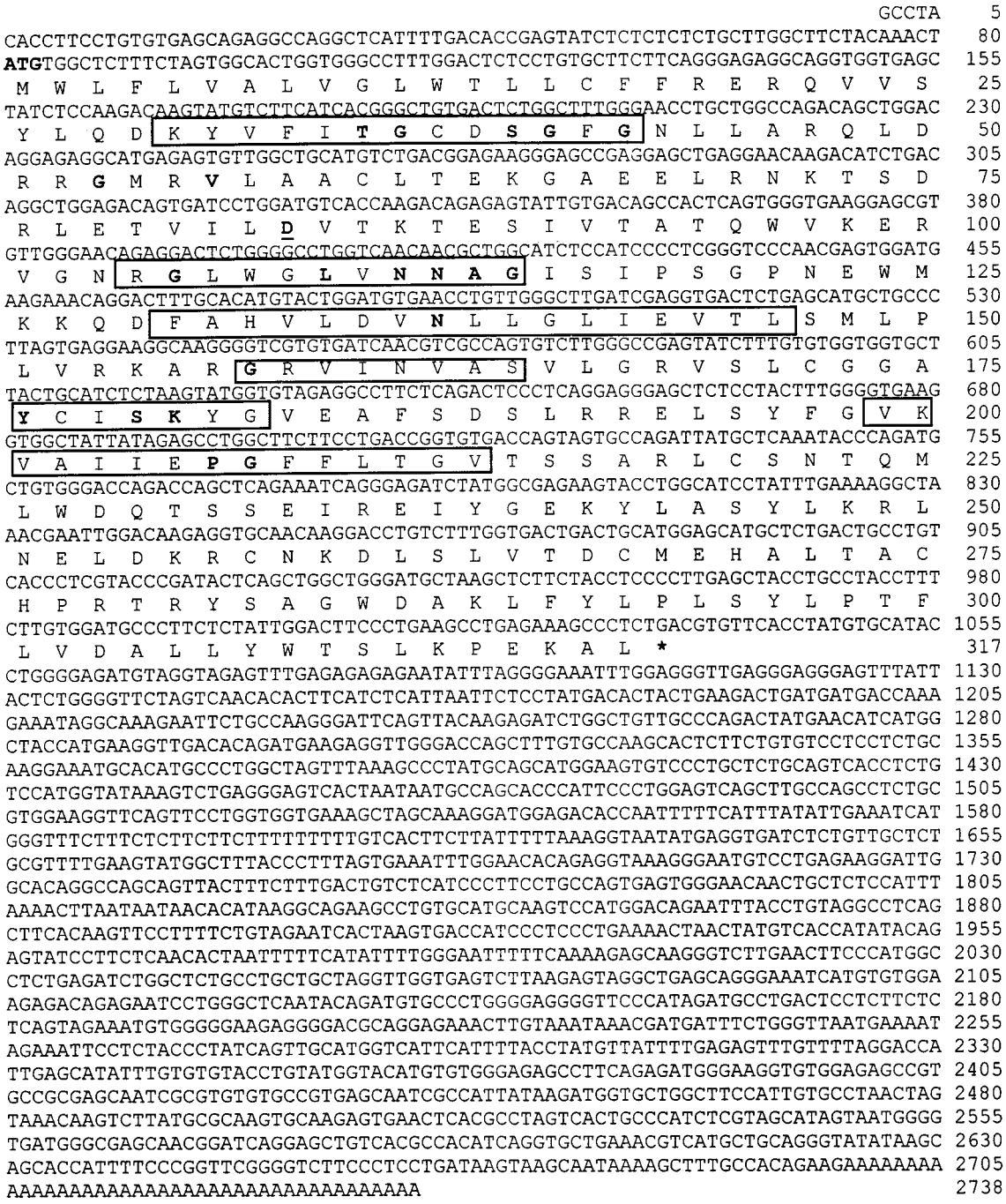

FIGURE 1: Nucleotide and deduced amino acid sequences of CRAD3. Boldface indicates the start codon and an asterisk denotes the stop codon. Boldface also indicates the amino acids that are conserved in most SDR family members. The boxed areas indicate the six motifs characteristic of steroid/retinoid metabolizing SDR (*12*).

RNA without reverse transcription was subjected to the same PCR reactions and program used for CRAD3.

RESULTS

cDNA and Amino Acid Sequences. To isolate a genomic clone of a mouse ortholog of rat RoDH2, a 129 SvJ mouse genomic DNA library was screened with a probe homologous among rat RoDH1, 2, and 3 (nucleotides 11−384 of RoDH2). One of the five plaques identified was analyzed. It contained a nucleotide sequence identical to part of an insert in an EST clone. The EST contained 5′-UTR, the entire coding region, and the entire 3′-UTR of an uncharacterized SDR. The first 1300 base pairs of the 3′-UTR had 85% identity with CRAD1, but the last 400 base pairs had only 25% identify with CRAD1. The coding region of this EST was used to construct pcDNA3/CRAD3, which has a deduced amino acid sequence that contains the six motifs characteristic of retinoid/steroid metabolizing SDR (*12*) and 20 of the 23 residues conserved in 70−90% of SDR (*13*). These include the cofactor-binding residues $TG^{36}(X)_3GXG$, the $G(X)_3L^{109}XNNAG$ motif, and the catalytic residues $S^{164}(X)_{11}Y(X)SK$ (Figure 1). The SDR was closest in amino acid identity and similarity with mouse CRAD1 and rat RoDH2 but had less similarity with other SDR that metabolize retinoids and androgens (Table 1, Figure 2). Each of the enzymes in Table 1, however, has different substrate

Table 1: Amino Acid Homologies and Retinol Preferences of SDR That Catalyze Retinoid and Steroid Metabolism

species	enzyme	amino acid homology		retinol specificity
		% identity	% similarity	
mouse	CRAD3	100	100	11-*cis* ≥ 9-*cis* (no *all-trans* activity)
mouse	CRAD1	95	98	11-*cis* ≅ 9-*cis* (weak *all-trans* activity)
mouse	RDH1	89	93	*all-trans* > 9-*cis*
rat	RoDH2	85	90	*all-trans* > 9-*cis*
mouse	CRAD2	81	89	11-*cis* active (weak *all-trans* and 9-*cis*)
rat	RoDH1	80	87	*all-trans* > 9-*cis*
rat	RoDH3	80	87	*all-trans* > 9-*cis*
mouse	RDH4	51	66	11-*cis* ≅ 9-*cis* (weak) ≥ *all-trans*

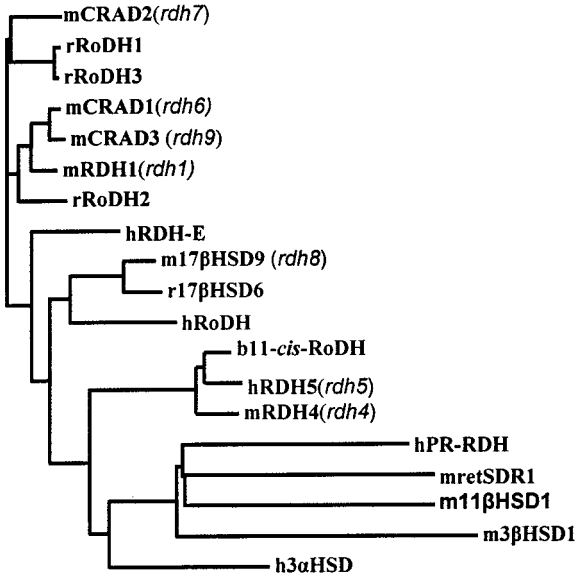

FIGURE 2: Evolutionary relationships among mammalian SDR that catalyze retinoid and steroid metabolism. The abbreviations used are (b) bovine, (h) human, (m) mouse, and (r) rat. m17βHSD9 and r17βHSD6 are not orthologs, whereas mRDH5, mRDH4, and b11-*cis*-RoDH are orthologs. hRoDH does not appear to be an ortholog of rRoDH or mRDH1.

specificities, despite similar amino acid sequences (*14*−*20*, *23*−*28*).

Enzymatic Activity. The supernatant of CHO cells transfected with pcDNA3/CRAD3 was used in a screen to identify candidate substrates, with arbitrarily chosen amounts of protein and time, and 2 mM NAD^+. The respective retinol substrates (5 μM) generated 11-*cis*-retinal (1000 ± 16) (pmol/assay ± SD, $n = 3$), 9-*cis*-retinal (496 ± 16), and 13-*cis*-retinal (100 ± 8). No *all-trans*-retinal production was detected from *all-trans*-retinol under the same conditions. With 3-adiol and androsterone (5 μM each), 1000 pmol of DHT and 2000 pmol of androstanedione, respectively, were generated (average of duplicates). No detectable products were generated from testosterone, DHT, estradiol, or corticosterone. A supernatant of CHO cells transfected with pcDNA3 alone (mock transfection) did not produce detectable products from the retinoid or steroid substrates assayed. This substrate specificity indicated that the cDNA encodes a SDR with *cis*-retinol/androgen dehydrogenase activity (i.e., CRAD3). CRAD3 functioned with either 2 mM NAD^+ or $NADP^+$, respectfully, generating 502 ± 21 (pmol/assay ± SD, $n = 3$) and 332 ± 37 of 9-*cis*-retinal from 5 μM 9-*cis*-retinol. An increase of pH increased activity until a plateau was reached at pH 8 (Figure 3). Activity at pH 7.4 was 82% of the activity at pH 8.

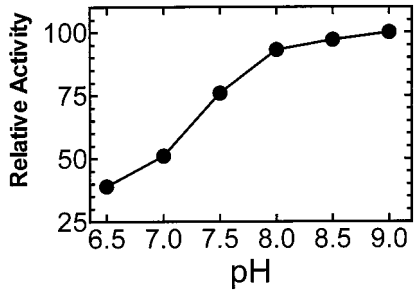

FIGURE 3: pH effects on CRAD3 activity. 9-*cis*-Retinal production was measured from 5 μM 9-*cis*-retinol with 20 μg of protein for 10 min.

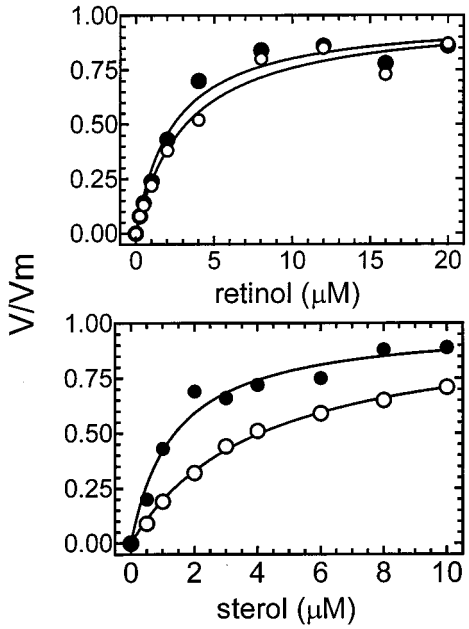

FIGURE 4: Kinetics of CRAD3. Graphs show representative data from the most active retinol and sterol substrates: (top panel) 11-*cis*-retinol (filled circles), 9-*cis*-retinol (open circles); (bottom panel) 3-adiol (filled circles), androsterone (open circles). Data show representative curves. Each experiment was done twice with 2−3 replicates per point.

The four most active substrates were evaluated in detail under linear velocity conditions (Figure 4). CRAD3 exhibited Michaelis−Menten kinetics for 9-*cis*-retinol, 11-*cis*-retinol, 3-adiol, and androsterone with K_m values of 2−4 μM (Table 2). To compare directly the activity of CRAD3 to that of CRAD1, side-by-side transfections were done and were normalized for transfection efficiencies. CRAD1 produced 31 ± 0.9 nmol/min/mg protein of 9-*cis*-retinal from 7 μM 9-*cis*-retinol (mean ± SD, $n = 4$), whereas CRAD3 produced 23 ± 0.9 nmol/min/mg under identical conditions. The $K_{0.5}$ values of CRAD1 and CRAD3 (5.4 and 3.6 μM, respectively)

Table 2: CRAD3 Substrate Specificities

substrate	product	activity	K_m (μM)	V_m (relative %)	V_m/K_m
11-*cis*-retinol	11-*cis*-retinal	*cis*-RDH	2.3[a]	113	17
3-adiol	DHT	3α-HSD	1.5	54	13
9-*cis*-retinol	9-*cis*-retinal	*cis*-RDH	3.6	100	10
androsterone	androstandione	3α-HSD	4.0	93	8
all-trans-retinol	none detected	*trans*-RDH			
testosterone	none detected	17β-HSD			
DHT	none detected	17β-HSD			
estradiol	none detected	17β-HSD			
corticosterone	none detected	11β-HSD			

[a] K_m and V_{max} values represent the averages of two determinations. Duplicate values were generally less than 10% from the average. V_m were normalized to a relative value of 100 for the V_m of CRAD3 with 9-*cis*-retinol (35 nmol/min/mg of protein). V_m/K_m were normalized relative to the calculated value of 10 with 9-*cis*-retinol (see text).

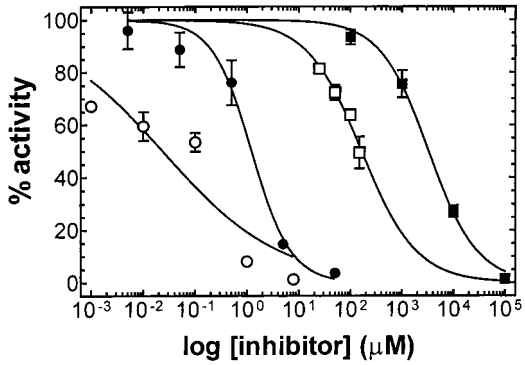

FIGURE 5: Inhibitors of CRAD3 activity. Reactions were run for 5 min with 8 μM 9-*cis*-retinol. Compounds assayed included 3-adiol (open circles), carbenoxolone (filled circles), ethanol (open squares), and 4-methylpyrazole (filled squares). Data bracket the 50% inhibition points and are the means ± SD of triplicates. The IC_{50} values were calculated by nonlinear regression analyses.

allow for calculations [V_m = rate x ($K_{0.5}$ + S)/S] from these rate data of 55 and 35 nmol/min/mg of protein for the V_m values of CRAD1 and CRAD3, respectively (*16*). CRAD1 and CRAD3, therefore, have nearly equivalent catalytic efficiencies ($V_m/K_{0.5}$) of ~10 for 9-*cis*-retinol.

Inhibitors of CRAD3. Competition between 9-*cis*-retinol and 3-adiol was examined, along with the effects of several alcohol dehydrogenase inhibitors (Figure 5). 3-Adiol inhibited 9-*cis*-retinal production with an IC_{50} value ~0.02 μM. Carbenoxolone also inhibited potently, with an IC_{50} value ~1.2 μM. Ethanol had an IC_{50} value ~170 μM, and 4-methylpyrazole inhibited CRAD3 with an IC_{50} value ~3.3 mM.

Tissue Distribution of CRAD3 mRNA. Northern blot hybridization revealed intense expression of CRAD3 mRNA in liver and much less intense expression in kidney tissue (Figure 6). The liver expressed a major 3 kb mRNA and a minor 3.7 kb mRNA. The kidney expressed only the 3.7 kb mRNA. No signal was observed by northern blotting in the other tissues assayed under these conditions. The more sensitive technique of RT-PCR was applied to determine whether other tissues express CRAD3 mRNA at lower levels than in the liver and kidney. CRAD3 mRNA was amplified by RT-PCR from multiple mouse tissues (testis, lung, small intestine, heart, and brain), with the liver and kidney showing the strongest signals.

CRAD3 Can Contribute to 9cRA Biosynthesis from 9-cis-Retinol in Intact Cells. To determine whether CRAD3 can contribute to 9cRA biosynthesis in intact cells, CHO cells

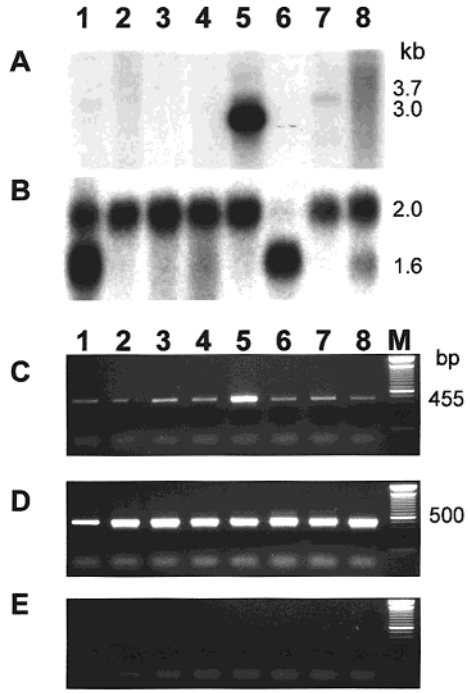

FIGURE 6: CRAD3 mRNA tissue expression. Northern blot hybridization (A and B) or PCR (C, D, and E) was done with poly-(A^+)mRNA from (1) heart, (2) brain, (3) spleen, (4) lung, (5) liver, (6) skeletal muscle, (7) kidney, and (8) testis: (A and C) probes or primers for CRAD3, (B and D) probes or primers for actin, (E) PCR with mRNA and CRAD3 primers.

were transfected with pcDNA3/CRAD3 along with vectors that encode three mouse RALDH: AHD2/RALDH1, RALDH2, and ALDH12 (Figure 7). Cells transfected with pcDNA3 alone (mock), with pcDNA3/CRAD3 alone, or with any of the three RALDH-expressing vectors alone produced no detectable 9cRA (data not shown). Cells cotransfected with CRAD3 and any one of the three RALDH isozymes produced 9cRA. AHD2, the mouse ortholog of the rat enzyme RALDH1, seemed somewhat more efficient than mouse RALDH2 for 9cRA biosynthesis in conjunction with CRAD3. The mouse ortholog of human ALDH12, however, seemed less efficient than ADH2 and RALDH2.

DISCUSSION

Although enzymes in the subgroup of mouse SDR that oxidize retinoids (CRAD1−3 and RDH4) share high amino acid conservation, they have substantial differences in substrate efficiencies. The newly characterized CRAD3 represents a retinoid SDR with relatively high efficiency for

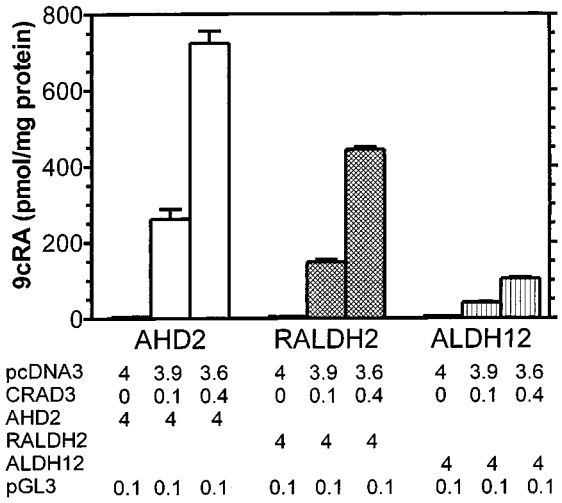

FIGURE 7: Biosynthesis of 9cRA catalyzed by CRAD3 and RALDH isozymes in intact cells. CHO cells were transfected with two amounts of pcDNA3/CRAD3 and fixed amounts of AHD2 (open bars), pcDNA3/RALDH2 (filled bars), or pcDNA3/ALDH12 (striped bars). Numbers indicate the amounts (μg) of vectors added to each plate. The vector pGL3 also was added as an aid to normalize transfection efficiency.

9-*cis*-retinol (V/K_m = 10 nmol/min/mg)/μM), similar to the value for CRAD1 (*Rdh*6). In comparison, RDH4 (*Rdh*4) has a V/K_m value of 0.007 (more than 1400-fold lower) for 9-*cis*-retinol, and CRAD2 (*Rdh*7) is inefficient and not saturable kinetically with 9-*cis*-retinol (*16*, *17*, *27*). Although all recognize multiple substrates, CRAD3 is the only one that does not recognize *all-trans*-retinol and, therefore, discriminates most between 9-*cis*- and *all-trans*-retinol. All have appreciable activity with 11-*cis*-retinol except CRAD2, but 11-*cis*-retinol does not occur extraoccularly (*16*−*20*, *23*−*28*). A likely retinoid substrate for CRAD3 and 1, therefore, appears to be 9-*cis*-retinol, at least outside of the retina. In addition, CRAD3 is much less efficient than CRAD1 as a 3α-HSD. CRAD3 has a greater $K_{0.5}$ (1.5 μM) with 3-adiol than does CRAD1 (0.2 μM) and a lower V_m value, yielding a $V/K_{0.5}$ value ~55-fold less than that of CRAD1 for 3-adiol (*16*). Thus, CRAD3 shows much higher activity than RDH4 for 9-*cis*-retinol, is more discriminating for retinoid versus steroids than CRAD1, and, unlike CRAD1, has no detectable activity with *all-trans*-retinol.

CRAD1 and 3 have different, but partially overlapping, mRNA expression patterns. CRAD3 shows marked expression in liver, with less intense expression in kidney and low levels of expression in testis, lung, intestine, heart, and brain. Other than liver, only kidney expresses CRAD1 intensely, and low levels of expression are detectable only in small intestine and heart. Most intense expression of CRAD1 and 3 in liver and kidney seems consistent with a function in 9cRA biosynthesis, because these two tissues reportedly have higher concentrations of 9-*cis*-retinol than other tissues (*29*, *30*). The mouse embryo and brain express RDH4, but whether other tissues do seems uncertain because of potential probe nonspecificity (*17*). Many tissues express the human ortholog of RDH4 (i.e., RDH5, but with low intensity relative to the eye (*25*)). The abundance of RDH4/5 in the eye suggests that it generates 11-*cis*-retinal in the visual cycle, but its relatively low expression outside of the eye and its inefficiency for 9-*cis*-retinol do not seem compatible with a function in 9cRA biosynthesis (*31*, *32*).

Cotransfections of CRAD3 with AHD2/RALDH1, RALDH2, and ALDH12 showed that CRAD3 generates 9-*cis*-retinal that is accessible to RALDH in intact cells and, therefore, could participate in 9cRA biosynthesis in vivo. The generation of lesser 9cRA from the CRAD3/ALDH12 pair as compared to the CRAD3/AHD2 and CRAD3/RALDH2 pairs was not foreseen, because its V/K_m values in vitro for 9-*cis*-retinal compare favorably with those of RALDH1 and RALDH2 (*22*). Perhaps preferential pairs of CRAD and RALDH form intracellularly. This possibility is under investigation.

Ethanol has profound pleiotropic effects, obscuring the mechanism whereby it interferes with CRAD3 (this work) and CRAD1 (*16*). Ethanol inhibition of both CRAD1 and 3, however, suggests that 9cRA biosynthesis may be compromised by intoxication. It remains to be determined whether this actually occurs in vivo. 4-Methylpyrazole, a prototypical inhibitor of the medium-chain alcohol dehydrogenases, also inhibits CRAD1 and CRAD3. 4-Methylpyrazole inhibits ADH class I potently and ADH class IV moderately, with K_i values from 0.1 to 2 μM and from 10 to 1500 μM, respectively, depending on the species (*13*). Inhibition of CRAD by ethanol and 4-methylpyrazole demonstrates that neither xenobiotic has specificity for the medium-chain alcohol dehydrogenases. Use of neither would provide unequivocal evidence of medium-chain alcohol dehydrogenase catalyses of retinol activation in vivo. Carbenoxolone, the aglycone of the licorice constituent glycyrrhizin, inhibits many SDR, including 11β-HSD, 15-hydroxyprostaglandin dehydrogenase, rat RoDH1 and RoDH2, and CRAD1, in addition to CRAD3 (*32*−*35*). Inhibition of 11β-HSD2 results in high blood pressure, but the consequences are not clear for RDH/CRAD inhibition. Inhibition of RDH4 or CRAD1 might contribute to the transient blindness caused by excessive licorice consumption, however (*36*).

Function of CRAD3 in androgen metabolism seems improbable because other enzymes occur with higher efficiencies for 3-adiol and androsterone. These may include several 17β-HSD isozymes. 17β-HSD9, for example, has nearly equivalent 17β-HSD and 3α-HSD activities (*37*). A human RDH, more closely related to 17β-HSD than to RDH, also has substantial 17β-HSD activity (*11*). The human RDH-E, rat RoDH1 and 2, and CRAD1 and 2 also harbor much more efficient 17β-HSD activity than does CRAD3 (*38*, *39*). All are expressed in liver, many in kidney, and several in other tissues. Unless CRAD3 expresses in a locus unique from the others, its inefficiency for DHT metabolism would not allow it to compete favorably with the other enzymes.

In summary, this paper shows that CRAD3 functions in transfected cells with each of three known RALDH isozymes to convert 9-*cis*-retinol into 9cRA consistent with a possible function in vivo, discriminates much more than CRAD1 against *all-trans*-retinol and 3α-hydroxysteroids, and has a different pattern of mRNA expression than CRAD1. These data are consistent with a unique contribution of CRAD3 to 9cRA biosynthesis in vivo.

REFERENCES

1. Lotan, R. (1988) *Prog. Clin. Biol. Res. 259*, 261−271.
2. Wolf, G. (1984) *Physiol. Rev. 64*, 674−937.
3. Renaud, J. P., and Moras, D. (2000) Structural studies on nuclear receptors. *Cell. Mol. Life Sci. 57*, 1748−1769.

4. Glass, C. K., Rosenfeld, M. G., Rose, D. W., Kurokawa, R., Kamei, Y., Xu, L., Torchia, J., Ogliastro, M. H., and Westin, S. (1997) *Biochem. Soc. Trans. 25*, 602−605.
5. Nagpal, S., and Chandraratna, R. A. (2000) *Curr. Pharm. Des. 6*, 919−931.
6. Russell, D. W., and Wilson, J. D. (1994) *Annu. Rev. Biochem. 63*, 25−61.
7. Wilson, J. D., and Gloyna, R. E. (1970) *Recent Prog. Horm. Res. 26*, 309−336.
8. Giffin, J. E., McPhaul, M. J., Russell, D. W., and Wilson, J. D. (1995) in *The Metabolic and Molecular Basis of Inherited Disease* (Scriver, C. R., Beaudet, A. L., Sly, W. S., and Valle, D., Eds.), pp 2967−2998, McGraw-Hill, New York.
9. Beaulieu, M., Lévesque, E., Hum, D. W., and Bélanger, A. (1996) *J. Biol. Chem. 271*, 22855−22862.
10. Bruchovsky, N. (1971) *Endocrinology 89*, 1212−1222.
11. Biswas, M. G., and Russell, D. W. (1997) *J. Biol. Chem. 272*, 15959−15966.
12. Bailey, T. L., Baker, M. E., and Elkan, C. P. (1997) *J. Steroid Biochem. Mol. Biol. 62*, 29−44.
13. Jörnvall, H., Persson, B., Krook, M., Atrian, S., Gonzàlez-Durate, R., Jeffery, J., and Ghosh, D. (1995) *Biochemistry 34*, 6003−6013.
14. Napoli, J. L. (2000) *Prog. Nucleic Acid Res. 63*, 139−188.
15. Napoli, J. L. (2001) *Mol. Cell. Endocrinol. 171*, 103−109.
16. Chai, X., Zhai, Y., and Napoli, J. L. (1997) *J. Biol. Chem. 272*, 33125−33131.
17. Su, J., Chai, X., Kahn, B., and Napoli, J. L. (1998) *J. Biol. Chem. 273*, 17910−17916.
18. Romert, A., Tuvendal, P., Simon, A., Dencker, L., and Eriksson, U. (1998) *Proc. Natl. Acad. Sci. U.S.A. 95*, 4404−4409.
19. Driessen, C. A., Winkens, H. J., Kuhlmann, E. D., Janssen, A. P., van Vugt, A. H., Deutman, A. F., and Janssen, J. J. (1998) *FEBS Lett. 428*, 135−140.
20. Mertz, J. R., Shang, E., Piantedosi, R., Wei, S., Wolgemuth, D. J., and Blaner, W. S. (1997) *J. Biol. Chem. 272*, 11744−11749.
21. El Alkawi, Z., and Napoli, J. L. (1994) *Biochemistry 33*, 1938−1943.
22. Lin, M., and Napoli, J. L. (2000) *J. Biol. Chem. 275*, 40106−40112.
23. Chai, X., Zhai, Y., Popescu, G., and Napoli, J. L. (1995) *J. Biol. Chem. 270*, 28408−28412.
24. Bradford, M. M. (1976) *Anal. Biochem. 72*, 248−254.
25. Wang, J., Eriksson, U., and Napoli, J. L. (1999) *Biochem. J. 338*, 23−27.
26. Gamble, M. V., Shang, E., Zott, R. P., Mertz, J. R., Wolgemuth, D. J., and Blaner, W. S. (1999) *J. Lipid Res. 40*, 2279−2292.
27. Gamble, M. V., Mata, N. L., Tsin, A. T., Mertz, J. R., and Blaner, W. S. (2000) *Biochim. Biophys. Acta 1476*, 3−8.
28. Zhang, M., Chen, W., Smith, S. M., and Napoli, J. L. (2001) *J. Biol. Chem. 276*, 44083−44090.
29. Heyman, R. A., Mangelsdorf, D. J., Dyck, J. A., Stein, R. B., Eichele, G., Evans, R. M., and Thaller, C. (1992) *Cell 68*, 397−406.
30. Paik, J., Vogel, S., Piantedosi, R., Sykes, A., Blaner, W. S., and Swisshelm, K., (2000) *Biochemistry 39*, 8073−8084.
31. Simon, A., Hellman, U., Wernstedt, C., and Eriksson, U. (1995) *J. Biol. Chem. 270*, 1107−112.
32. Driessen, C. A. G. G., Janssen, B. P. M., Winkens, H. J., van Vugt, A. H. M., de Leeuw, T. L. M., and Janssen, J. J. M. (1995) *Invest. Ophthamol. Visual Sci. 36*, 1988−1996.
33. Boerman, M. H. E. M., and Napoli, J. L. (1995) *Biochemistry 34*, 7027−7037.
34. Mantero, F., Palermo, M., Petrelli, M. D., Tedde, R., Stewart, P. M., and Shackleton, C. H. (1996) *Steroids 61*, 193−196.
35. Duax, W. L., and Ghosh, D. (1998) *Endocr. Res. 24*, 521−529.
36. Dobbins, K. R., and Saul, R. F. (2000) *J. Neuro-Ophthalmol. 20*, 38−41.
37. Su, J., Lin, Min, and Napoli, J. L. (1999) *Endocrinology 140*, 5275−5284.
38. Gough, W. H., Van Ooteghem, S., Sint, T., and Kedishvili, N. Y. (1998) *J. Biol. Chem. 273*, 19778−19785.
39. Jurukovski, V., Markova, N. G., Karaman-Jurukovska, N., Randolph, R. K., Su, J., Napoli, J. L., and Simon, M. (1999) *Mol. Gen. Metab. 67*, 62−73.

BI0119316